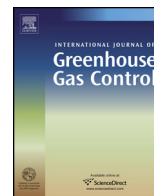




Originally published as:

Lueth, S., Ivanova, A., Kempka, T. (2015): Conformity assessment of monitoring and simulation of CO<sub>2</sub> storage: A case study from the Ketzin pilot site. - *International Journal of Greenhouse Gas Control*, 42, p. 329-339.

DOI: <http://doi.org/10.1016/j.ijggc.2015.08.005>



## Conformity assessment of monitoring and simulation of CO<sub>2</sub> storage: A case study from the Ketzin pilot site



Stefan Lüth<sup>a,\*</sup>, Alexandra Ivanova<sup>a</sup>, Thomas Kempka<sup>b</sup>

<sup>a</sup> GFZ German Research Centre for Geosciences, Centre for Geological Storage CGS, Germany

<sup>b</sup> GFZ German Research Centre for Geosciences, Section 5.3 – Hydrogeology, Germany

### ARTICLE INFO

#### Article history:

Received 10 March 2015

Received in revised form 8 June 2015

Accepted 7 August 2015

#### Keywords:

CO<sub>2</sub> plume

Seismic monitoring

Reservoir simulation

Conformance

Performance criteria

### ABSTRACT

Demonstrating conformity between observed and simulated plume behaviour is one of the main high-level requirements, which have to be fulfilled by an operator of a CO<sub>2</sub> storage site in order to assure safe storage operations and to be able to transfer liability to the public after site closure. The observed plume behaviour is derived from geophysical and/or geochemical monitoring. Repeated 3D seismic observations have proven to provide the most comprehensive image of a CO<sub>2</sub> plume in various projects such as Sleipner, Weyburn, or Ketzin. The simulated plume behaviour is derived from reservoir simulation using a model calibrated with monitoring results. Plume observations using any monitoring method are always affected by limited resolution and detection ability, and reservoir simulations will only be able to provide an approximated representation of the occurring reservoir processes. Therefore, full conformity between observed and simulated plume behaviour is difficult to achieve, if it is at all. It is therefore of crucial importance for each storage site to understand to what degree conformity can be achieved under realistic conditions, comprising noise affected monitoring data and reservoir models based on geological uncertainties. We applied performance criteria (plume footprint area, lateral migration distance, plume volume, and similarity index) for a comparison between monitoring results (4D seismic measurements) and reservoir simulations, considering a range of seismic amplitude values as noise threshold and a range of minimum thickness of the simulated CO<sub>2</sub> plume. Relating the performance criteria to the noise and thickness threshold values allows assessing the quality of conformance between simulated and observed behaviour of a CO<sub>2</sub> plume. The Ketzin site is provided with a comprehensive monitoring data set and a history-matched reservoir model. Considering the relatively high noise level, which is inherent for land geophysical monitoring data, a reasonable conformance between the observed and simulated plume behaviour is demonstrated.

© 2015 The Authors. Published by Elsevier Ltd. This is an open access article under the CC BY license (<http://creativecommons.org/licenses/by/4.0/>).

### 1. Introduction

On the European and international level, there is a variety of regulations defining the legal framework for CO<sub>2</sub> storage in the six lifecycle phases of a storage site: (1) assessment, (2) characterization, (3) development, (4) operation, (5) post closure, and (6) post transfer (Kühn et al., 2013). These phases are separated by project or regulatory milestones. According to EU/UK regulations, “post closure” and “post transfer” phases are defined as follows. The post closure phase begins at the end of the injection (“operation”) (Korre, 2011) and comprises also the transfer of liability from the operator

to the public. The “post transfer” phase is the (indefinite) period after the operator has transferred responsibility to the competent authorities.

The transitions from operation to post closure and from post closure to post transfer are crucial moments for the operator, but in particular also for the regulators as well as for the general public. According to the EU CCS Directive, Article 18, the site operator has to demonstrate that three high-level requirements are fulfilled in order to assure the long-term safety of the storage site and to be able to transfer the liability to the public. These high-level criteria are:

1. Monitored and simulated CO<sub>2</sub> migration are in conformity.
2. There is no leakage detected.
3. The CO<sub>2</sub> plume is stable or evolves towards stability.

\* Corresponding author at: GFZ German Research Centre for Geosciences, Telegrafenberg, 14473 Potsdam, Germany.

E-mail address: [slueth@gfz-potsdam.de](mailto:slueth@gfz-potsdam.de) (S. Lüth).

The term “CO<sub>2</sub> plume” refers to the free phase CO<sub>2</sub> injected into a storage formation. Conformity demonstration (1) is commonly achieved by comparing reservoir monitoring parameters with history-matched flow simulations. Monitoring parameters to be matched may be the lateral extent of the topmost CO<sub>2</sub> layer, observed by seismic measurements and simulated by flow simulations (Chadwick and Noy, 2010). If the CO<sub>2</sub> arrival times in monitoring wells and reservoir pressures are observed in the injection and monitoring wells, matching these observations with flow simulations indicates that the existing reservoir model and governing reservoir processes are reasonably well understood for the monitored reservoir compartment (Kempka and Kühn, 2013; Kempka et al., 2013b). Field studies at the Sleipner and Ketzin storage sites have shown that during the course of a project, as more monitoring data becomes available, a better match between monitoring data and reservoir simulations may be achieved (Holloway et al., 2013; Chadwick and Noy, 2015). However, perfect matching is almost impossible to achieve due to various limitations, which are related to model resolution, model parameters, observational limitations and other uncertainties (Oreskes et al., 1994). Therefore, it is important for any specific site to understand the characteristics of the monitoring data and the reservoir model. Questions to be addressed are: What are the minimal spatial dimensions of CO<sub>2</sub> detected by the applied monitoring methods? Do baseline and monitoring observations allow calibrating and verifying a maximum realistic reservoir model and to what degree is it possible to achieve conformance between simulated and observed reservoir processes?

Proving the absence of any detectable leakage (2) is a challenge for monitoring technologies, generally based on repeated geophysical surveys or geochemical observations (e.g. Giese et al., 2009). There are various geophysical techniques available, including relatively cost-efficient approaches such as 4D gravity, vertical seismic profiling (VSP) or crosswell electromagnetics, as well as geochemical tracer monitoring in observation wells, allowing for quantitative tracking of the CO<sub>2</sub> distribution (Michael et al., 2010). These methods, however, are restricted to relatively small areas defined by the distances between the injection and monitoring wells. For large scale commercial storage projects and in the likely absence of a network of monitoring wells, priority will be given to 4D seismic, which proved as a successful monitoring tool in the scope of the Sleipner (Chadwick et al., 2009) or Ketzin (Ivanova et al., 2012) as well as various other CO<sub>2</sub> injection projects (e.g. White, 2013). The detection threshold of 4D seismic monitoring depends on repeatability noise and is highly site-specific (Chadwick et al., 2014).

The evolution of a storage site towards a stable situation (3) depends on several trapping processes acting at different time scales. These are structural and stratigraphic trapping, residual trapping, dissolution in the brine, as well as mineral trapping by geochemical fluid/mineral reactions and precipitation of minerals (“SRDM”, IPCC, 2005; Frykman, 2012). The highest stability, and thus highest storage safety, results from mineralization of the injected carbon dioxide, which is, on the other hand, the slowest process. According to coupled reservoir simulations, a significant amount of injected CO<sub>2</sub> can be expected to be mineralized at the Ketzin pilot site within 10,000 years (De Lucia et al., 2015; Kempka et al., 2013a, 2014; Klein et al., 2013). The quantitative contribution of mineralization to stabilizing a storage complex is highly site-specific and hydro-chemical simulations indicate a high degree of uncertainty, due to assumptions made with respect to intra-reservoir heterogeneities (Estublier et al., 2013) and the parameterization of the geochemical system (De Lucia et al., 2015).

The “conformity” criterion (1) can be regarded as the governing criterion, which is implicitly included in the “no leakage” (2) and the “stability” (3) criteria. If the operator is not able to demonstrate conformity between simulation and monitoring data, the

reservoir model used for simulations does not provide a reasonably realistic framework for site behaviour assessment, possibly due to insufficient knowledge about the reservoir, or the applied monitoring techniques are inappropriately applied. In either case, regulating authorities, and the general public have no reason to assume that under such circumstances the operator will be able to demonstrate fulfilment of the “no leakage” criterion. Further, the demonstration of long-term stability is currently mainly based on reservoir simulations, involving the four trapping mechanisms. If short and intermediate term simulations do not demonstrate conformity with monitoring data, they will not be able to provide a reliable prediction of reservoir stabilization in the long term. Therefore, it is important to understand the significance of the conformity requirement in relation to the real conditions present at storage sites. Monitoring techniques are characterized by detection limits and reservoir models are always built on the basis of limited geological knowledge about the reservoir. This needs to be quantified for each site in order to perform a realistic assessment of the conformance between monitored and simulated plume behaviour.

The Ketzin pilot site for CO<sub>2</sub> storage offers a rich portfolio of monitoring data, and is provided with relatively well constrained geological data as a basis for the reservoir model (Giese et al., 2009; Norden and Frykman, 2013; Martens et al., 2013). In this study, we use the high-resolution 3D seismic monitoring data and reservoir simulations based on a revised reservoir model version (Kempka et al., 2013b) in order to investigate, if and to what degree conformity between monitoring and simulation can be achieved. The reservoir simulation results for autumn 2009 and 2012 are presented in Fig. 1 (lower panel) in terms of thickness maps of the free-phase CO<sub>2</sub>. For the monitoring and simulation performed on the Sleipner project (Chadwick and Noy, 2010), Chadwick and Noy (2015) suggested a number of different geometrical features of the monitored and simulated CO<sub>2</sub> plumes to be compared. For our Ketzin case study, we have slightly modified these geometrical features for a quantitative comparison between monitoring results and simulations. We used the performance parameters plume footprint area, maximum lateral migration distance, and plume volume. These parameters compare geometrical properties of the lateral and vertical CO<sub>2</sub> distribution in the reservoir, without directly comparing the true shapes of the plumes. In addition, we also compared the true shapes of observed and simulated plumes by using the similarity index, relating the observed and simulated plume areas with the overlapping area.

## 2. Geophysical monitoring at the Ketzin pilot site

The Ketzin pilot site for CO<sub>2</sub> storage has been the first European onshore storage site (Würdemann et al., 2010; Martens et al., 2013). The site is located approximately 25 km west of Berlin and Potsdam in the Federal State of Brandenburg in Germany. From June 2008 through August 2013, 67 kt of CO<sub>2</sub> were injected into sandstone layers within the Upper Triassic Stuttgart Formation, at 630–650 m depth (Martens et al., 2014). The injection well was drilled on the southern flank of a double anticlinal structure (Roskow–Ketzin–Anticline), with the top of the anticline located approximately 1.5 km north of the injection, forming a natural structural trap for the injected CO<sub>2</sub>. A comprehensive and multi-disciplinary monitoring programme has been established on the site (Giese et al., 2009; Martens et al., 2013), a crucial part of which is 3D time-lapse seismic monitoring (Juhlin et al., 2007; Ivanova et al., 2012; Ivandic et al., 2015). The data set consists, to date, of one baseline and two repeat survey campaigns. The baseline survey was acquired in summer/autumn 2005 (Juhlin et al., 2007). The acquisition area covered approximately 12 km<sup>2</sup>, including the injection site and the top of the anticlinal structure, which is expected to

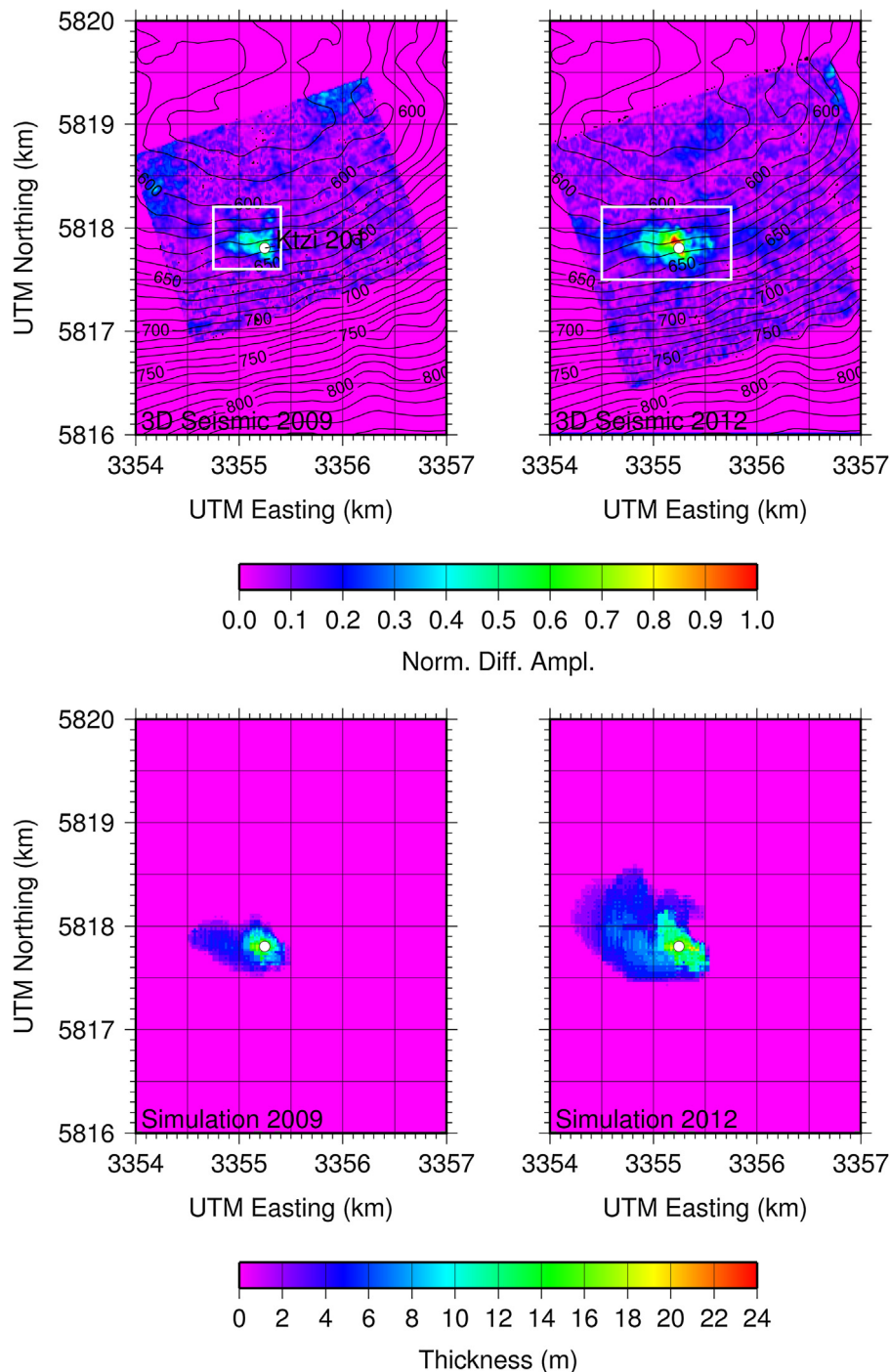


**Fig. 1.** Normalized amplitude difference maps for 2009 and 2012 surveys indicating the lateral extent of free phase  $\text{CO}_2$  detected by seismic measurements (upper panels). Depth contour lines indicating the topography of the storage formation with the anticline top ca. 1.5 km north of the injection well (Norden and Frykman, 2013). The injection well (“Ktzi 201”) is indicated by a white dot in all maps. White rectangles indicate the area, which has been excluded for the analysis of noise amplitude distribution (Fig. 2). Reservoir simulations were performed to predict the distribution of  $\text{CO}_2$  for 2009 and 2012. The thickness of the simulated  $\text{CO}_2$  plume is indicated in the lower panels for 2009 (left) and 2012 (right), respectively.

be the final location of the injected and up-dip migrating carbon dioxide. 14 months after injection started and after 22 kt had been injected, the acquisition of the first repeat survey began in September 2009, covering approximately  $7 \text{ km}^2$  around the injection site. The second 3D seismic repeat survey was acquired in summer/autumn 2012, with 61 kt injected. All three surveys were acquired using the same acquisition geometry (detailed description in Juhlin et al., 2007), only the number of templates was varied according to the respective acquisition areas. After an initial

pilot survey investigated different sources and receiver systems (Yordkayhun et al., 2009), an accelerated weight drop had been chosen (Bison EWG III) as a seismic source for all surveys. The acquisition geometry had been planned to enable a nominal 25-fold subsurface coverage with a common midpoint (CMP) bin size of 12 m by 12 m. This fold was reached in some parts of the acquisition area (Juhlin et al., 2007), but due to logistical restrictions in parts of the area, the fold was reduced to coverage values between 5 and 10 at some locations with likely adverse effects on data quality.

The processing of the three data sets was done by using identical workflows and parameters. In order to maximize repeatability of fold and azimuthal coverage, for the time-lapse analysis of the baseline and the two repeat surveys, source and receiver positions common for the considered surveys were used, respectively. The seismic data sets underwent a time-lapse cross-equalization workflow using Hampson Russell's Pro4D software (Ivanova et al., 2012). After the cross-calibration of the seismic subvolumes, the repeatability was assessed by computing the normalized root mean square (NRMS) difference between the subvolumes, which is commonly used as a metric for comparing seismic traces, and which is sensitive to differences in timing, phase and amplitude behaviour. Values between 0.2 and 0.4 were determined for most of the areas, indicating good repeatability for onshore time-lapse measurements, with higher values (indicating worse repeatability) at the margins of the acquisition area and close to the injection site, where CO<sub>2</sub> injection related amplitude changes reduced repeatability. In order to image the seismic signature of the CO<sub>2</sub> propagation in the reservoir, the seismic volumes were subtracted (base – repeat 1 and base – repeat 2) and the amplitude variation in the depth level of the reservoir extracted. The maps of normalized time-lapse difference amplitudes for the first and second repeat surveys are shown in Fig. 1 (upper panels). Both maps show a clear amplitude anomaly concentrated around the injection well, with high normalized difference amplitude values. The anomalies show an irregular shape, with strong azimuthal variation in lateral extent from the injection well, which is interpreted as an indication of the internal heterogeneity of the storage formation (Norden and Frykman, 2013). The anomalies further indicate that the focus of the CO<sub>2</sub> footprint is situated in northwestern direction from the injection well, although, according to the topography gradient of the reservoir formation, a mostly northward-directed CO<sub>2</sub> propagation from the injection well was expected.

In previous studies, the amplitude anomaly maps were used as a basis for a quantitative assessment of the spatial carbon dioxide distribution (Ivanova et al., 2012; Ivandic et al., 2015). The time-lapse seismic data, pulsed-neutron-gamma logging results (Baumann et al., 2014), and petrophysical core measurements (Kummerow and Spangenberg, 2011) were integrated in order to estimate the mass of injected carbon dioxide imaged by the seismic repeat data. For the first repeat survey, the mass estimation was summed up to 20.5 kt, which is approximately 7% less than what had been injected (Ivanova et al., 2012). For the second repeat survey, the mass estimation was summed up to approximately 10–15% less than what had been injected (Ivandic et al., 2015). The relatively large deviation may be explained by several factors of uncertainty, discussed in detail in Ivanova et al. (2012), and by partial dissolution of the injected CO<sub>2</sub>, thus reducing the amount of free CO<sub>2</sub>, which can be detected by seismic time-lapse observations. These quantitative assessment studies have shown that conformity between injected and estimated CO<sub>2</sub> quantities can only be achieved with some degree of uncertainty, which needs to be quantified for a realistic assessment of conformity studies. Due to the uncertainties related to detectability issues, incompletely quantified dissolution contributions, as well as uncertainties about the physical state of the CO<sub>2</sub> in the reservoir (Ivanova et al., 2013), a quantitative assessment of full-scale storage reservoirs is not necessarily an appropriate measure for demonstrating regulatory conformance of the storage complex. On the other hand, the quantitative estimation may be a viable technique to be applied on detected leakages, where a small amount of CO<sub>2</sub> may have migrated out of the storage formation and may have accumulated in a secondary aquifer.

The assessment of conformity between monitored and expected behaviour will be more informative when the monitoring data and reservoir simulations, considering data and model related uncertainties as well as governing reservoir processes, are integrated into

one analysis. In this study we present an approach we applied on the monitoring and simulation results of the Ketzin pilot site, taking into account uncertainties related to the identification of the CO<sub>2</sub> distribution from the monitoring data and related to the detection limits, affecting the ability to image the full extent of the CO<sub>2</sub> plume.

### 3. Conformity study

#### 3.1. Introduction to performance criteria

For the conformance assessment of seismic monitoring results and reservoir simulations, we use the following performance criteria, some of which were previously suggested and investigated for monitoring results of the Sleipner storage site (Holloway et al., 2013; Chadwick and Noy, 2015): The plume footprint area, the lateral migration distance, the plume volume, and the similarity index of the simulated and observed plumes. The assessment is based on a crucial assumption regarding the general conformance behaviour of simulated and observed CO<sub>2</sub> plumes. Simulation and geophysical observations are subject to numerical and physical limitations. As for the reservoir simulations, numerical descriptions of the reservoir model will never be able to provide a fully realistic model, as the model is based on limited observations (from a few wells or surface measurements with limited resolution) and a fully realistic reservoir model would exceed currently available capacities of modelling and computing systems. However, if a history-matched reservoir model has been elaborated based on seismic data and reservoir monitoring, the simulated CO<sub>2</sub> distribution may be assumed to sufficiently well represent the realistic situation in the reservoir. It is assumed that the simulated plume footprint area and the simulated plume volume predicted by reservoir simulations on the basis of history-matched models are in conformance with the “real” (and in fact unknown) CO<sub>2</sub> distribution, even if the exact shape of the CO<sub>2</sub> plume cannot be reproduced by the simulation. Geophysical monitoring data, on the other hand are characterized by limited spatial resolution related to the finite wavelength of the seismic signal used, and by reduced detection capabilities due to the presence of time-lapse noise in the observations. It can therefore be assumed that the geophysical signature of the CO<sub>2</sub> plume, in terms of the areal extent, and/or the volumetric distribution of the CO<sub>2</sub> will detect a part of the full plume, which is characterized by a certain minimum thickness threshold. Comparing the performance measures of the geophysical signature, assuming a range of noise thresholds, with the performance measures of the simulated CO<sub>2</sub> plume will enable to determine the site-specific achievable conformance between simulated and observed plumes and the detection limits of the geophysical measurements considered in this context.

##### 3.1.1. Plume footprint area

This criterion describes the areal extent of the CO<sub>2</sub> plume, that is the area of the reservoir where partial (or full) saturation of free phase CO<sub>2</sub> is present. For the reservoir simulation, this is equivalent to the area within the plume outline on a horizontal plane. For the seismic monitoring, the plume footprint area is the area of the seismic time-lapse amplitudes above the noise level, indicating a time-lapse signature of the plume. The normalized seismic difference amplitudes range between “0” and “1”, with “1” indicating the highest amplitude difference between the monitoring and baseline measurements (Fig. 1). The actual size of the seismically detected plume is strongly dependent on the definition of the noise level within the seismic data and on detection limits of the seismic time-lapse observations. In order to take into account the uncertainties related to the seismic plume footprint area, we consider the seismic plume footprint area in dependence from various

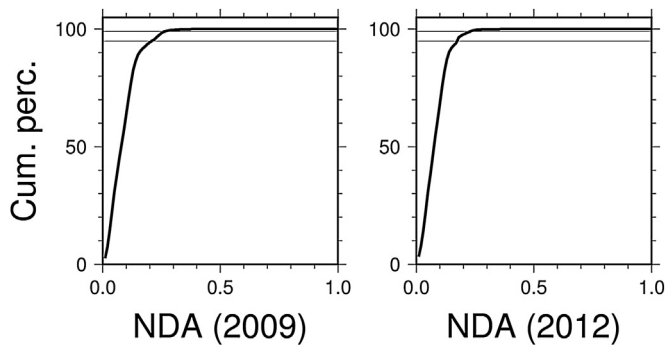


**Fig. 2.** Cumulative percentile of noise amplitude values (NDA: normalized differential amplitude) in the time-lapse amplitude map for the top of the storage formation in the 2009 data set (left) and in the 2012 data set (right). The 95% and 99% levels are marked by horizontal lines, respectively.

threshold levels, including low normalized amplitudes (noise) and larger normalized amplitudes, which are related to CO<sub>2</sub> saturation. We analyzed the distribution of the normalized amplitude difference values for the 2009 repeat data set. We assumed that the (seismic) CO<sub>2</sub> plume was constrained within the white rectangle shown in Fig. 1 and the area outside of this rectangle was noise. The cumulative distribution of amplitude values for the noise area is plotted in Fig. 2. It shows that 95% of all noise amplitude values are below 0.2, and 99% of all values are below 0.27 in the 2009 data set. In the 2012 data set, 95% of all noise amplitudes are below 0.18, and 99% are below 0.23. Allowing a small percentage of “outliers” in the noise area, we here assume that normalized amplitude difference values of 0.2 and higher can be attributed to the CO<sub>2</sub> signature, with increasing probability for the amplitude range between 0.2 and 0.3 (99.7% of all noise amplitude values range below 0.3), and with a slightly higher probability of a lower noise threshold amplitude for the 2012 data.

Some parts of the simulated CO<sub>2</sub> plume are characterized by low thickness, of a few decimetres to metres, which is below the seismic detection limit. Therefore, we consider the simulated plume footprint area for various detection limits, from 0 m (the whole plume) up to 12 m minimum thickness (which is above the detection limit and should describe an area, which is smaller than the seismically determined plume footprint).

### 3.1.2. Maximum lateral migration distance

This criterion describes, like the footprint area, the lateral extent of a CO<sub>2</sub> plume in the reservoir, but together with a comparison of the footprint area also allows to assess the degree of anisotropy. If a reservoir model does not describe correctly the degree of anisotropy of fluid flow parameters, the plume footprint area may show good conformance between observed and simulated plumes, but the lateral migration distances may differ significantly between simulation and monitoring data. The maximum lateral migration distance has been investigated for amplitude thresholds in the seismic data and for minimum thickness thresholds in the simulation. For the seismic data, the radius of investigation was restricted to 500 m (2009) and 1000 m (2012) around the injection point. This restriction was introduced in order to exclude individual high amplitude noise patches, which can be found in the seismic amplitude distributions in marginal regions of the acquisition area. These small and isolated high amplitude patches can be attributed to be residual time-lapse noise, which is not related to any injected CO<sub>2</sub>.

### 3.1.3. Plume volume

The plume volume describes the total volume of the reservoir rocks affected by partial or full CO<sub>2</sub> saturation. For the reservoir simulation, the plume volume is the total volume of all model

elements, which are affected by (partial or full) CO<sub>2</sub> saturation. For the seismic monitoring results, the plume volume is computed via the surficial area of CDP bins with time-lapse amplitude values above the defined threshold and the thickness of the CO<sub>2</sub> reservoir for each considered CDP bin, using the time-delay of reflections below the reservoir relative to reflections above the reservoir (Ivandić et al., 2015). The thickness of the CO<sub>2</sub> affected reservoir can be computed according to

$$H = \Delta T \frac{V_1 V_2}{2(V_1 - V_2)}, \quad (1)$$

where  $H$  is the thickness of the CO<sub>2</sub> plume,  $\Delta T$  is the time-delay of between reflections from above and below the reservoir comparing baseline and monitoring data,  $V_1$  is the P-wave velocity in the brine saturated reservoir, and  $V_2$  is the P-wave velocity in the CO<sub>2</sub> saturated reservoir, with CO<sub>2</sub> saturations derived from PNG logging and the P-wave velocity derived from a rock physical model based on laboratory measurements (Ivandić et al., 2015).

### 3.1.4. Similarity index

Whereas the previous performance parameters provide a quantitative measure of conformance between monitoring and simulation results without considering the “true” shapes of the simulated and observed plumes, the similarity index specifically measures how much the shape of the monitored plume resembles the shape of the simulated plume. We use the Sørensen–Dice coefficient, which had been initially established to compare ecological community data (Dice, 1945). It reads:

$$S = \frac{2 * C}{A + B}. \quad (2)$$

In our case,  $A$  and  $B$  are the plume footprint areas of monitored and simulated CO<sub>2</sub> distribution, and  $C$  is the intersecting area of both plumes. If  $A$  and  $B$  are identical,  $S = 1$ . If  $A$  and  $B$  do not overlap at all, or one of either  $A$  or  $B$  is extremely small compared to the other,  $S$  is equal to or tending to zero.

## 3.2. Results

### 3.2.1. Plume footprint area

The results of the footprint area analysis are shown in Fig. 3. Two panels show the analysis performed for 2009 (first monitoring survey) and for 2012 (second monitoring survey). For autumn 2009, reservoir simulation predicted a plume footprint area of 418,000 m<sup>2</sup>, with approximately 50% of the areal extent of the plume thinner than 3.5 m (Fig. 3, upper panel, black curve). A small proportion of the plume area (6%) is 10 m thick or thicker. The areal extent of the seismic anomaly, attributed to the CO<sub>2</sub> plume, is analyzed for a range of noise threshold values between 0.12 and 0.4, where 0.12 is within the range of time-lapse noise values (see Figs. 1 and 2) and 0.4 is within the range of CO<sub>2</sub> signature amplitude values. The footprint area of the seismic plume ranges from 1.19 Million m<sup>2</sup> for a normalized amplitude threshold of 0.12–42,000 m<sup>2</sup> for a normalized amplitude threshold of 0.4. Given the distribution of normalized amplitude values for the areas identified as noise reference areas (Fig. 2), we may assume that a realistic noise threshold value for the considered seismic amplitude distribution is between 0.2 and 0.27, i.e. amplitude values below this noise threshold are attributed to noise, amplitude values above this noise threshold are attributed to the presence of CO<sub>2</sub>. The distribution of noise amplitude values shows somewhat similar behaviour for the 2009 and 2012 data sets, with slightly higher concentration on lower values for the 2012 data set. As these differences are small, we discuss the results on the basis of identical threshold values for both data sets. For noise threshold values between 0.2 and 0.27, the seismic plume footprint area ranges between 357,000 m<sup>2</sup> and 128,000 m<sup>2</sup>,

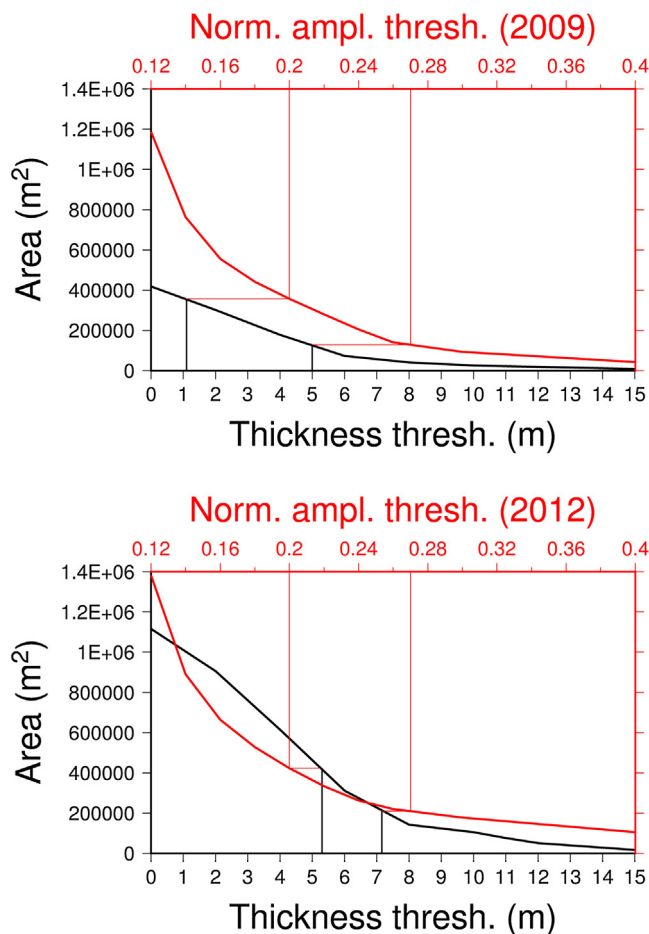


**Fig. 3.** Plume footprint area curves from reservoir simulations (black) and seismic monitoring (red). Vertical black lines indicate equivalent thickness thresholds determined for a noise threshold range between 0.2 and 0.27. For both noise values, the seismic plume footprint areas are determined (horizontal red lines). The equivalent thickness threshold is determined by the thickness threshold value at which the horizontal red line crosses the black curve (simulated plume footprint area versus thickness threshold).

which is between 85% and 30% of the full simulated plume footprint area. For the following consideration this assumption is made: Even if the reservoir model cannot represent a fully realistic parameter distribution for the storage reservoir, it is based on a realistic physical representation of fluid flow, considered in the dynamic reservoir simulations. As a consequence, we assume that the simulated plume footprint conforms to the real CO<sub>2</sub> plume area, and the distribution of thickness variations within the plume are described realistically by the reservoir simulation. Under this assumption, we can estimate an “equivalent thickness threshold” as shown in Fig. 3. The size of the seismic plume footprint area for the noise range between 0.2 and 0.27 is equivalent to a proportion of the simulated plume with minimum thickness of 1.1 m (noise threshold 0.2) to 5.0 m (noise threshold 0.27).

For autumn 2012 (Fig. 3, lower panel), reservoir simulation predicted a plume footprint area of 1.11 Million m<sup>2</sup>. The seismic plume footprint ranges from 423,000 m<sup>2</sup> (noise threshold 0.2) to 210,000 m<sup>2</sup> (noise threshold 0.27), which is between 39% and 19% of the full simulated plume footprint area. The size of the seismic plume footprint area for the noise range between 0.2 and 0.27 is equivalent to a proportion of the simulated plume with minimum thickness of 5.3 m (noise threshold 0.2) to 7.2 m (noise threshold 0.27).

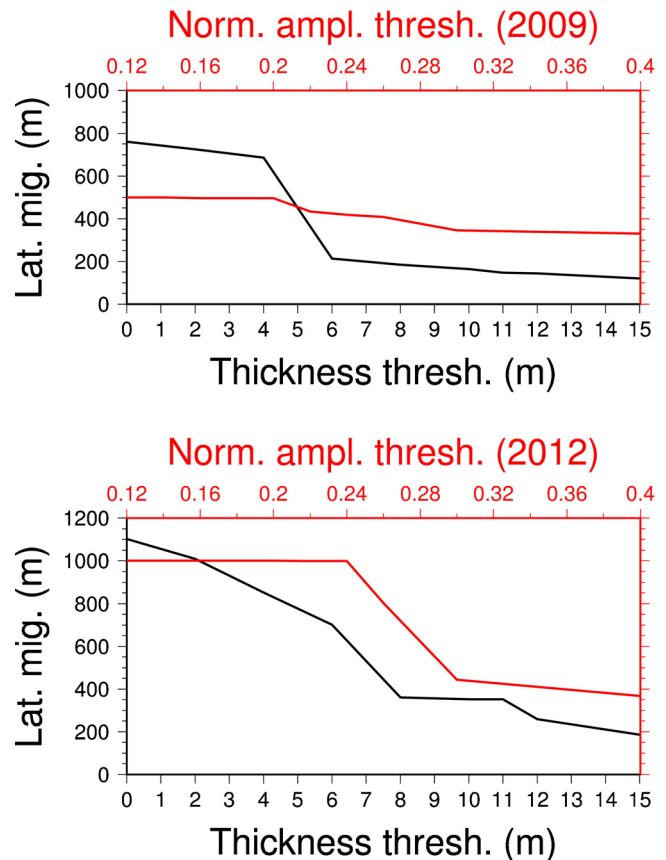


**Fig. 4.** Maximum lateral migration distance of simulated (black) and observed (red) CO<sub>2</sub> plumes for 2009 (top) and 2012 (bottom). Due to high amplitude noise at the margins of the seismic data, distances larger than 500 m (2009) and 1000 m (2012) were discarded.

### 3.2.2. Maximum lateral migration distance

The maximum lateral migration distance derived from observed and simulated CO<sub>2</sub> plumes is shown in Fig. 4. The simulated CO<sub>2</sub> plume has migrated up to 760 m (2009) and 1100 m (2012) from the injection well. The maximal distances could not be considered in the seismic time-lapse amplitude distribution maps, which contain isolated high amplitude noise patches at a range of distances. Therefore, the investigation radius for the seismic data was restricted to 500 m for the 2009 data set and to 1000 m for the 2012 data set. In the 2009 data, the lateral migration distance of the observed plume is fixed at 500 m for amplitude threshold values below 0.2 (noise level), and decreases exactly from the values of 0.2 upward. The migration distance maintains a still relatively high level (340 m) up to amplitude threshold of 0.4 showing the lateral extent of the central part of the seismically detected plume (Fig. 1). The 2012 data are characterized by lower signal to noise ratio, compared to the 2009 data, which is also reflected in the results shown here (Fig. 4, bottom).

The investigation of the 2012 data set was restricted to a radius of 1000 m, and only at a relatively large amplitude threshold of 0.24, a dependency of amplitude thresholds and migration distance can be identified. From a comparison of the plume footprint area, we conclude that the 2012 seismic data set probably detects the part of the CO<sub>2</sub> plume, which is at least 5.3 m thick. From a comparison with the lateral migration distance curves in Fig. 4, we can see that the simulated plume with a minimum thickness of 5.3 m has a simulated lateral migration distance of 750 m. However, the seismic data suggest a detected lateral migration distance larger than 1000 m, then decreasing at larger time-lapse amplitude thresholds. This observation may either indicate that

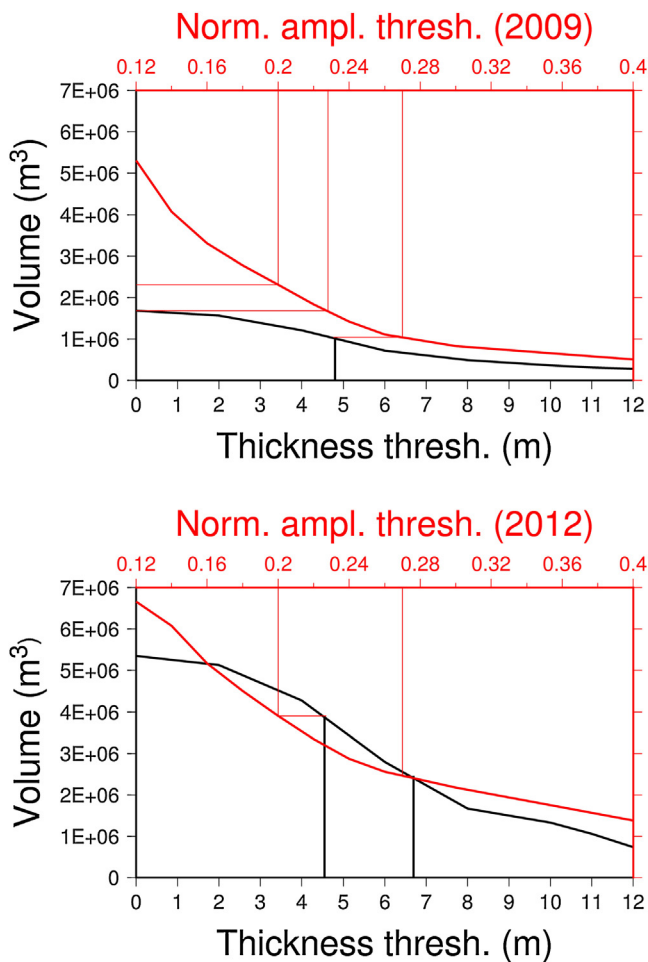


**Fig. 5.** Plume volume curves from reservoir simulations (black) and seismic monitoring (red). Vertical black lines indicate equivalent thickness thresholds determined for a noise threshold range between 0.2 and 0.27. For both noise values, the seismic volumes are determined (horizontal red lines). The equivalent thickness threshold is determined by the thickness threshold value at which the horizontal red line crosses the black curve (simulated plume volume versus thickness threshold). In the 2009 data set, the plume volume is overestimated for a noise threshold of 0.2.

the seismic data significantly overestimate the lateral migration of the plume, or that the noise level of the amplitude data is too high to achieve a stable result of the lateral migration distance, which holds for both the 2009 and 2012 data sets.

### 3.2.3. Plume volume

The results of the plume volume analysis are displayed in Fig. 5. Two panels show the analysis performed for 2009 (first monitoring survey) and for 2012 (second monitoring survey). For autumn 2009, reservoir simulation predicts a gaseous CO<sub>2</sub> plume volume of  $1.68 \times 10^6 \text{ m}^3$ , with approximately 50% of the plume volume being thinner than 5.5 m (Fig. 5, upper panel, black curve). 22% of the plume volume is at least 10 m thick. The seismic plume volume is analyzed for a range of noise threshold values as for the plume footprint area (normalized amplitude values from 0.12 to 0.4). We consider noise threshold values between 0.2 and 0.27 as realistic thresholds, separating noise from the CO<sub>2</sub> signature. For these noise threshold values, the seismic plume volume ranges between  $2.3 \times 10^6 \text{ m}^3$  (overestimating the full simulated plume volume) and  $1.04 \times 10^6 \text{ m}^3$  (62% of full simulated plume volume). Equivalently to the considerations made for the plume footprint area, we estimated the “equivalent thickness threshold” (black vertical lines

in Fig. 5), ranging between 0 m and 4.8 m for the data and simulation results for autumn 2009.

For autumn 2012, reservoir simulation predicted a plume volume of  $5.35 \times 10^6 \text{ m}^3$ . The seismic plume volume ranges from  $3.9 \times 10^6 \text{ m}^3$  (0.2) to  $2.46 \times 10^6 \text{ m}^3$  (0.27) which is between 73% and 46% of the full simulated plume volume. These size values are equivalent to a proportion of the simulated plume volume with minimum thickness of 4.5 m (noise threshold 0.2) to 6.7 m (noise threshold 0.27).

### 3.2.4. Similarity index

The results of the similarity index computed for the seismic and simulated CO<sub>2</sub> plumes are shown in Fig. 6. The similarity index has been computed, after re-gridding the simulated plume footprint and the seismic amplitude data onto the same equidistant 2D grid ( $1 \text{ m} \times 1 \text{ m}$ ). For the seismic data, the plume footprint with threshold values between 0.12 and 0.8, and for the simulated plume, thickness threshold values between zero (full plume) and 15 m were used. For the 2009 and 2012 data sets, the similarity index ranges between zero (no overlap) and 0.7. The maximum similarity index of 0.7 can be attributed, according to Equation (2), to different scenarios. The end-members of these are: (1) Both footprint areas are of identical size. Then, the overlapping area of both is 70% of the full plume area. (2) One of the plume footprint areas is smaller than the other, and located completely within the area of the larger plume. The larger plume area exceeds the smaller one by a factor of 1.85, so the larger plume is almost twice as large as the smaller one.

For the 2009 data set, maximum values of the similarity index have been computed for seismic amplitude thresholds between 0.35 and 0.45, and for thickness threshold values between 6.5 m and 10 m. Obviously, the best match between seismic and simulated plumes is reached, if concentrating on the part of the plume thicker than at least 6.5 m. This relates to the part of the plume, which is situated in relatively close vicinity to the injection location, whereas the huge majority of the thinner parts of the plume are at distances larger than approximately 100–200 m from the injection well. A straightforward explanation can be given for this. The geological model, which was used to set up the reservoir model for the simulations, is best constrained where information from boreholes is available (Norden and Frykman, 2013). This is the case for the area around the injection well and the three monitoring wells at the Ketzin pilot site, which are distributed within a small area of approximately  $50 \text{ m} \times 100 \text{ m}$  west-east and south-north extension, respectively (Martens et al., 2013).

A somewhat similar observation is made on the 2012 data set (Fig. 6, right). Highest similarity index values are computed for seismic threshold values between 0.2 and 0.3, and for thickness thresholds between 6.5 m and 7 m. This is only a small range, compared to the results of the 2009 data set, providing a further indication of the lower signal-to-noise ratio of the 2012 seismic data, compared to the 2009 data, which is also reflected in the smaller proportion of seismic plume footprints, assuming the same noise thresholds as for the 2009 data set. Ivandic et al. (2015) pointed out that the second seismic repeat survey (2012) was characterized by larger deviations in source-receiver geometry from the baseline data than the first one. Although large efforts were made to reduce time-lapse noise in the data, this may at least partially explain the smaller similarity index values in the optimal range, compared to the 2009 data. A maximum similarity index of at least 0.6 is computed for a simulated plume of at least 5 m thickness and seismic plume footprint amplitudes larger than 0.2, also concentrating the maximum to the plume closest to the injection and monitoring wells of the Ketzin pilot site.



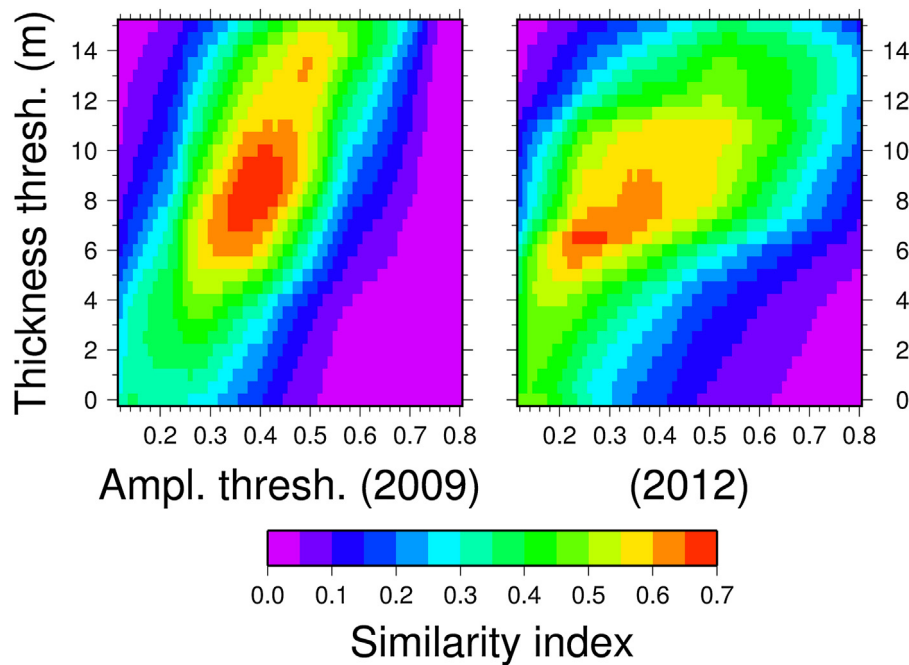


**Fig. 6.** Comparison of the seismic and simulated plume footprints, using the similarity index based on the Sørensen–Dice coefficient (see explanation in text). Left: Similarity index for seismic and simulated plume footprints in autumn 2009. Right: The same for autumn 2012.

#### 4. Discussion

The results of the seismic time-lapse monitoring and reservoir simulations of CO<sub>2</sub> injection at the Ketzin pilot site for CO<sub>2</sub> storage have been used for an investigation of different performance parameters. These performance parameters are crucial for the assessment of CO<sub>2</sub> storage sites at all stages, but especially in a relatively mature state, when the transfer of responsibility to the public is approaching. We considered performance parameters, which are mainly based on geometrical investigations of seismic time-lapse amplitudes and reservoir simulation results. Petrophysical relations and the varying saturation of CO<sub>2</sub> within the reservoir were not taken into account. The *plume footprint area* compares the areal extent of the observed plume (by seismic measurements) with the simulated plume. Due to the presence of time-lapse noise in the seismic data, and due to physical limitations, the seismic data have a detection threshold related to the thickness (and saturation) of the CO<sub>2</sub> distribution in the reservoir. If we assume the simulated plume footprint area to conform to real conditions, without necessarily describing the exact CO<sub>2</sub> plume in the reservoir correctly, the seismic data of the first repeat survey 2009 are able to detect up to 85% of the injected CO<sub>2</sub> plume area. At least 61,000 m<sup>2</sup> of the plume remain undetected. For the second repeat survey (2012), the same investigation suggested that only up to 39% of the CO<sub>2</sub> plume was detected, and at least 687,000 m<sup>2</sup> remain undetected, if the reservoir simulations predicted correctly the relatively large extent of CO<sub>2</sub> distribution within a thin layer.

The investigation of the *lateral migration distance* was affected by the residual time-lapse noise in the seismic amplitude maps. The time-lapse noise needed to be as much as possible excluded from an automated investigation, and thus could only be restricted to relatively high amplitude threshold values, in particular for the 2012 data set. In the 2009 data, the lateral migration distance derived from the seismic amplitude map, conforms well to a part of the simulated plume of approximately 5 m thickness. In the 2012 data, the lateral migration distance derived from the seismic amplitude map seems to overestimate the plume, when considering a detection threshold of approximately 5 m thickness. Given the noise

level in the seismic time-lapse amplitude maps, an automated computation of the lateral migration distance tends to provide rather unstable results as even smallest (but high amplitude) noise patches may affect the assessment. The same high amplitude patches would also be included in an analysis of the plume footprint area or volume, but their contribution to these parameters would be much smaller than for the lateral migration distance. Using the lateral migration distance as a performance parameter will be possible only after some interpretative processing of the seismic time-lapse amplitude maps in the presence of residual time-lapse noise.

The *plume volume* adds the thickness of the CO<sub>2</sub> plume to the previously discussed plume footprint area. The results of this comparison suggest that the seismic data of the first repeat survey (2009) detect the full plume volume (if assuming that the simulated plume volume conforms to the real plume volume). Considering a finite detection threshold, it may be assumed that the plume volume determined from the seismic data is rather slightly overestimated relative to the real CO<sub>2</sub> plume volume in 2009. Plume footprint area and plume volume do not show the same degree of conformance between seismic data and reservoir simulation results which might be expected due to almost similar approaches to compute these performance parameters. However, the plume volume, derived from seismic monitoring data, uses assumptions on CO<sub>2</sub> saturation distribution and on the validity of a petrophysical model which are difficult to calibrate and are therefore characterized by a high degree of uncertainty. In addition, the traveltime push-down of reflections below the reservoir ( $\Delta T$  in Eq. (1)) is an unstable parameter in noisy data possibly adding an additional bias to the estimation. For the 2012 data, at least  $1.45 \times 10^6$  m<sup>3</sup> remain undetected, compared to the simulated plume volume, which implies that approximately 73% of the plume volume is detected.

A measure for the conformance of the plume shapes can be acquired via the *similarity index*, relating the areal extent of the plumes and the overlapping area. The observed and simulated plumes were compared, considering amplitude and thickness thresholds within a wide range of values (Fig. 6). In the 2009 data set, the best conformance between observed and simulated plumes reached 0.7 for a rather small proportion of the plumes

(amplitude threshold larger than 0.3, thickness threshold larger than 6.5 m). Considering noise threshold values between 0.2 and 0.27 (as discussed for the seismic time-lapse amplitude maps), optimal thickness thresholds (in terms of maximum similarity indices) are in the range of 1–5 m, which is comparable to the results of the plume footprint area investigation for the 2009 data set. The similarity index map for the 2012 data set (Fig. 6, right) confirms the observations made for the previously discussed performance parameters. Maximum similarity index values of 0.7 have been found for a very small parameter range only. On the other hand, intermediate values are distributed over a larger range of values, compared to the 2009 data set. The main reason for this is the larger lateral extent of the simulated and observed CO<sub>2</sub> plumes in 2012. A larger extent of the plume (and larger thickness of the simulated plume) results also in a larger range of amplitude and thickness threshold values where proportions of the plume overlap; though, with only smaller proportions than when considering smaller plumes, which are concentrated more strongly in the vicinity of the injection well at the Ketzin pilot site.

The application of different performance parameters for the comparison of observed and simulated CO<sub>2</sub> distributions in the storage reservoir has shown that conformance between these parameters is affected by limited detection ability of the geophysical data and by reservoir models, which are unable to realistically represent the reservoir heterogeneity. The discussions on the plume footprint areas and the plume volumes have shown that significant relative deviations between simulated and observed CO<sub>2</sub> plumes were identified. The largest relative deviations were found in the study of the plume footprint area for the 2012 data set, where only 19% of the footprint area predicted by reservoir simulations would be detected under unfavourable conditions (high noise threshold).

The assessments of different performance parameters comparing monitoring and reservoir simulation results generally showed better conformance for the 2009 data set than for the more recent 2012 data set, which seems to contradict the concept of “predictive conformance”, demonstrated on the Sleipner case study (Chadwick and Noy, 2015). This concept consists in the expectation that conformance between simulations and monitoring increases with each update of the reservoir model by cumulatively incorporating most recent monitoring results into the static model. There is one main reason that this concept is not fulfilled in the present study, and this is related to a slightly different setup of the Ketzin case study compared to Sleipner. The reservoir simulations used for the Ketzin pilot site were based on a static reservoir model, which had been constructed incorporating the 2009 3D seismic data and any other observations made at the site thereafter. Thus, good conformance of the 2009 monitoring data with reservoir simulations for 2009 had to be expected, whereas reservoir simulations for 2012 were performed with much higher uncertainty about fluid flow parameters at larger distances from the injection well. Note that between 2009 and 2012, almost 40,000 tonnes of CO<sub>2</sub> were injected at Ketzin, which is almost twice as much as has been stored in 2009. It had to be expected that the ongoing migration of the CO<sub>2</sub> being continuously injected between 2009 and 2012 into a highly heterogeneous and small-scale reservoir structure would reach regions, which have not been imaged in terms of their fluid flow parameters by the first 3D seismic survey in 2009. Also, in 2009, a large part of the CO<sub>2</sub> plume concentrates relatively close to the injection site, including the injection well and two more monitoring wells within a radius of approximately 110 m. This part of the reservoir is well constrained, not only by seismic data, but also by detailed lithological and petrophysical information from the injection and monitoring wells (Norden and Frykman, 2013). Predicting the propagation of the CO<sub>2</sub> plume for distances farther away from the injection and monitoring wells of the Ketzin pilot site without

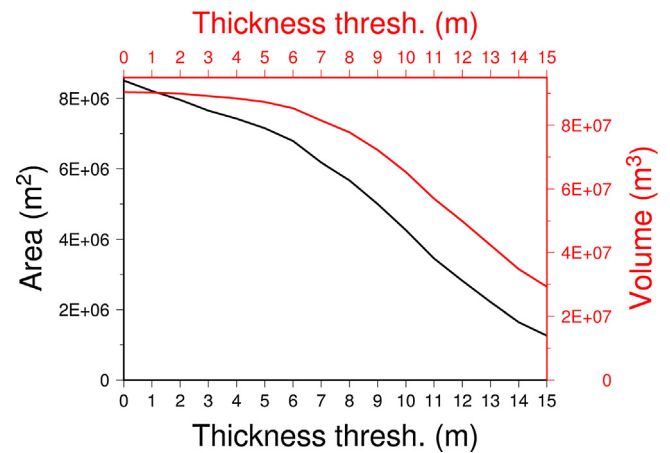


Fig. 7. Plume footprint area (black curve) and plume volume (red curve) for a hypothetical demonstration-scale CO<sub>2</sub> storage at the Ketzin pilot site, with 2.5 Million tonnes of CO<sub>2</sub> injected. Thickness threshold values between 0 m (full plume) and 15 m were considered.

geophysical constraints will evidently be based on a highly uncertain spatial distribution of fluvial sand channels in the Stuttgart Formation, and thus reduce conformance.

The high relative deviation between simulation and monitoring, which has been described above, would certainly be unacceptable for a large-scale storage site. However, it needs to be taken into account that this study has been performed on a data set acquired on a pilot site for CO<sub>2</sub> storage, which is characterized by extremely small amounts of CO<sub>2</sub> being injected over a relatively long period of time. Therefore, all geophysical monitoring methods applied on this site are operating close to the absolute detection threshold, in particular when considering that 4D seismic measurements on land are challenged by highly unfavourable time-lapse noise conditions. The undetected dimensions of the plume (687,000 m<sup>2</sup>, 1.45 × 10<sup>6</sup> m<sup>3</sup> for the 2012 data) reflect these problems in detecting those parts of the CO<sub>2</sub> plume, which are too thin to be determined under real time-lapse noise conditions. It is realistic to assume that these detectability conditions will be comparable for larger scale (demonstration or even full commercial scale) storage sites. In order to study the effect of upscaling the performance assessment done on the Ketzin pilot site data, demonstration-scale storage reservoir simulations were performed using the Ketzin reservoir model. 2.5 × 10<sup>6</sup> tonnes were injected into the storage formation. For this merely synthetic case, seismic data are not available, but the plume footprint area and the plume volume were derived for thickness detection threshold values, which are shown in Fig. 7. It is immediately clear that the plume footprint area and the plume volume increase more slowly with decreasing thickness thresholds, indicating a smaller proportion of the CO<sub>2</sub> distributed in very thin layers, compared to pilot scale storage. If we now assume a range of thickness detection threshold values (depending on real site conditions) between 4 and 7 m, undetected plume area ranges between 13% (4 m) and 28% (7 m), undetected volume ranges between 3% (4 m) and 10% (7 m). In absolute values, undetected area is between 1.08 × 10<sup>6</sup> m<sup>2</sup> and 2.32 × 10<sup>6</sup> m<sup>2</sup> (4 and 7 m, respectively), undetected volume ranges between 1.95 and 8.94 Million m<sup>3</sup>. These undetected plume footprint area and volume values are slightly larger than those estimated for the Ketzin case, but they still range in the same order of magnitude as the undetected areas and volumes for the 2012 observations and simulations at the Ketzin pilot site, where only 2.7% of the CO<sub>2</sub> has been injected, compared to the simulated demonstration scale.

## 5. Conclusions

In the present study, the comprehensive seismic monitoring data set and results of reservoir simulations of CO<sub>2</sub> storage at the Ketzin pilot site have been used to set up and apply performance parameters for assessing the conformance between observed and simulated CO<sub>2</sub> plume migration in the reservoir. Due to the small-scale of the CO<sub>2</sub> storage at Ketzin, geophysical monitoring from the surface has been able to detect the CO<sub>2</sub> injected in the reservoir, but the comparison of monitoring data and reservoir simulations suggests that a significant amount of CO<sub>2</sub>, residing in thin layer structures, remains undetected. This affects the maximum achievable conformance between the observed and simulated plume extent. For the plume footprint area, conformance between the observed area and the simulated (full plume footprint) area has reached 85% for the 2009 and 39% for the 2012 data sets. For the plume volume, better conformance between observed and simulated behaviour is observed, because undetected thin layer parts of the CO<sub>2</sub> reservoir do not contribute much to the volume of the full CO<sub>2</sub> plume. The performance criteria “plume footprint area” and “plume volume” have been proven as useful parameters in assessing the conformance between simulated and observed plume behaviour, provided that the detection threshold of seismic measurements is taken into account in the study. The “maximum lateral plume migration” is a parameter, which is difficult to derive from (noisy) seismic time-lapse amplitude maps, commonly used to derive the lateral extent of CO<sub>2</sub> reservoirs. If this parameter is to be used in addition to the plume footprint area and volume, it would be preferable to derive the lateral migration distance on an interpreted amplitude map, excluding small-scale but high-amplitude noise patches severely affecting the parameter.

Whereas the previously discussed performance parameters compare geometrical relations without considering the “real” shapes of the plumes, the similarity index, derived from the Sørensen–Dice coefficient (Eq. (2)), provides a quantitative measure for the areal overlap between observed and simulated plumes. An investigation of this parameter for the Ketzin pilot site has shown that a maximum “similarity” between simulated and observed plumes is achieved, when concentrating on thickness thresholds above 6.5 m and normalized amplitude thresholds from at least 0.2. These observations can be used as indicators of conformance quality between observed and simulated plumes. Conformance can be regarded as “high”, if the maximum similarity index is reached for small thickness threshold and amplitude threshold values. In addition, a high absolute value of the maximum similarity index needs to indicate that the shapes and propagation directions of the CO<sub>2</sub> plume conform for the observed and simulated plumes. A maximum similarity index of 0.7 for the Ketzin pilot site data and simulations may be regarded as a reasonable result, indicating that the greater part of the simulated and observed plumes overlap with each other. In the conformance assessment of larger-scale storage sites, this parameter will also be useful in showing the convergence between observed and simulated plume behaviour, by applying the same investigation to monitoring data in comparison with simulated plumes based on various realisations of reservoir models, starting with initial models set up in the early operational phase of a storage site and continuing with updated models after incorporating an increasing amount of monitoring data collected during the operational phase.

## Acknowledgements

The authors gratefully acknowledge the funding for the Ketzin project received from the European Commission (6th and 7th Framework Programme, projects CO<sub>2</sub>SINK, CO<sub>2</sub>CARE), two German ministries – the Federal Ministry of Economics and Technology and

the Federal Ministry of Education and Research – and industry since 2004. The ongoing R&D activities are funded within the project COMPLETE by the Federal Ministry of Education and Research. Further funding is received by VGS, RWE, Vattenfall, Statoil, OMV and the Norwegian CLIMIT programme. Two anonymous reviewers have provided highly constructive comments and suggestions that helped to improve the paper.

## References

- Baumann, G., Hennings, J., De Lucia, M., 2014. Monitoring of saturation changes and salt precipitation during CO<sub>2</sub> injection using pulsed neutron-gamma logging at the Ketzin site. *Int. J. Greenh. Gas Control* 28, 134–146.
- Chadwick, R.A., Noy, D., Arts, R., Eiken, O., 2009. Latest time-lapse seismic data from Sleipner yield new insights into CO<sub>2</sub> plume development. *Energy Procedia* 1 (1), 2103–2110.
- Chadwick, R.A., Noy, D.J., 2010. History-matching flow simulations and time-lapse seismic data from the Sleipner CO<sub>2</sub> plume. *Geol. Soc. Lond. Petrol. Geol. Conf. Ser.* 2010 7, 1171–1182, <http://dx.doi.org/10.1144/0071171>.
- Chadwick, R.A., Marchant, B.P., Williams, G.A., 2014. CO<sub>2</sub> storage monitoring: leakage detection and measurement in subsurface volumes from 3D seismic data at Sleipner. *Energy Procedia* 63, 4224–4239.
- Chadwick, R.A., Noy, D.J., 2015. Underground CO<sub>2</sub> storage: demonstrating regulatory conformance by convergence of history-matched modelled and observed CO<sub>2</sub> plume behavior using Sleipner time-lapse seismics. *Greenh. Gas. Sci. Technol.* 5, 1–17, <http://dx.doi.org/10.1002/ggh.1488>.
- De Lucia, M., Kempka, T., Kühn, M., 2015. A coupling alternative to reactive transport simulations for long-term prediction of chemical reactions in heterogeneous CO<sub>2</sub> storage systems. *Geosci. Model Dev.* 8, 279–294, <http://dx.doi.org/10.5194/gmd-8-279-201>.
- Dice, L.R., 1945. Measures of the amount of ecologic association between species. *Ecology* 26 (3), 297–302.
- Estublier, A., Fornel, A., Parra, T., Deflandre, J.-P., 2013. Sensitivity study of the reactive transport model for CO<sub>2</sub> injection into the Utsira saline formation using 3D fluid flow model history matched with 4D seismic. *Energy Procedia* 37, 3574–3582, <http://dx.doi.org/10.1016/j.egypro.2013.06.250>.
- Frykman, P., 2012. Review of relevant trapping mechanisms based on site portfolio. CO<sub>2</sub>CARE Publications, pp. 39, <http://dx.doi.org/10.2312/GFZ.CO2CARE.D3.1>.
- Giese, R., Hennings, J., Lüth, S., Morozova, D., Schmidt-Hattenberger, C., Würdemann, H., Zimmer, M., Cosma, C., Juhlin, C., CO<sub>2</sub>SINK Group, 2009. Monitoring at the CO<sub>2</sub>SINK site: a concept integrating geophysics, geochemistry and microbiology. *Energy Procedia* 1 (1), 2251–2259.
- Holloway, S., Chadwick, R.A., CO<sub>2</sub>CARE Group, 2013. Best practice guidelines. CO<sub>2</sub>CARE Deliverable D5.4, online: <http://www.co2care.org>
- IPCC, 2005. In: Metz, B., Davidson, O., de Coninck, H.C., Loos, M., Meyer, L. (Eds.), *IPCC Special Report on Carbon Dioxide Capture and Storage, Prepared by Working Group III of the Intergovernmental Panel on Climate Change*. Cambridge University Press.
- Ivancic, M., Juhlin, C., Lüth, S., Bergmann, P., Kashubin, A., Sopher, D., Ivanova, A., Baumann, G., Hennings, J., 2015. Geophysical monitoring at the Ketzin pilot site for CO<sub>2</sub> storage: new insights into the plume evolution. *Int. J. Greenh. Gas Control* 32, 90–105, <http://dx.doi.org/10.1016/j.ijggc.2014.10.015>.
- Ivanova, A., Kashubin, A., Juhojuntti, N., Kummerow, J., Hennings, J., Juhlin, C., Lüth, S., Ivancic, M., 2012. Monitoring and volumetric estimation of injected CO<sub>2</sub> using 4D seismic, petrophysical data, core measurements and well logging: a case study at Ketzin, Germany. *Geophys. Prospect.* 60, 957–973, <http://dx.doi.org/10.1111/j.1365-2478.2012.01045.x>.
- Ivanova, A., Juhlin, C., Lengler, U., Bergmann, P., Lüth, S., Kempka, T., 2013. Impact of temperature on CO<sub>2</sub> storage at the Ketzin site based on fluid flow simulations and seismic data. *Int. J. Greenh. Gas Control* 19, 775–784, <http://dx.doi.org/10.1016/j.ijggc.2013.05.001>.
- Juhlin, C., Giese, R., Zinck-Jørgensen, K., Cosma, C., Kazemeini, H., Juhojuntti, N., Lüth, S., Norden, B., Förster, A., 2007. 3D baseline seismics at Ketzin, Germany: the CO<sub>2</sub>SINK project. *Geophysics* 72 (5), B121–B132, <http://dx.doi.org/10.1190/1.2754667>.
- Kempka, T., Kühn, M., 2013. Numerical simulations of CO<sub>2</sub> arrival times and reservoir pressure coincide with observations from the Ketzin pilot site, Germany. *Environ. Earth Sci.* 70 (8), 3675–3685, <http://dx.doi.org/10.1007/s12665-013-2614-6>.
- Kempka, T., Klein, E., De Lucia, M., Tillner, E., Kühn, M., 2013a. Assessment of long-term CO<sub>2</sub> trapping mechanisms at the Ketzin pilot site (Germany) by coupled numerical modelling. *Energy Procedia* 37, 5419–5426, <http://dx.doi.org/10.1016/j.egypro.2013.06.460>.
- Kempka, T., Class, H., Görke, U.-J., Norden, B., Kolditz, O., Kühn, M., Walter, L., Wang, W., Zehner, B., 2013b. A dynamic flow simulation code intercomparison based on the revised static model of the Ketzin pilot site. *Energy Procedia* 40, 418–427, <http://dx.doi.org/10.1016/j.egypro.2013.08.048>.
- Kempka, T., De Lucia, M., Kühn, M., 2014. Geomechanical integrity verification and mineral trapping quantification for the Ketzin CO<sub>2</sub> storage pilot site by coupled numerical simulations. *Energy Procedia* 63, 3330–3338, <http://dx.doi.org/10.1016/j.egypro.2014.11.361>.
- Klein, E., De Lucia, M., Kempka, T., Kühn, M., 2013. Evaluation of long-term mineral trapping at the Ketzin pilot site for CO<sub>2</sub> storage: an integrative approach using

- geochemical modelling and reservoir simulation. *Int. J. Greenh. Gas Control* 19, 720–730, <http://dx.doi.org/10.1016/j.ijggc.2013.05.014>.
- Korre, A., 2011. CO<sub>2</sub>CARE Publications, <http://dx.doi.org/10.2312/GFZ.CO2CARE-D1.1>.
- Kühn, M., Wipki, M., Durucan, S., Korre, A., Deflandre, J.-P., Boulharts, H., Lüth, S., Frykman, P., Wollenweber, J., Kronimus, A., Chadwick, A., Böhm, G., CO<sub>2</sub>CARE Group, 2013. Key site abandonment steps in CO<sub>2</sub> storage. *Energy Procedia* 37, 4731–4740.
- Kummerow, J., Spangenberg, E., 2011. Experimental evaluation of the impact of the interactions of CO<sub>2</sub>–SO<sub>2</sub>, brine, and reservoir rock on petrophysical properties: a case study from the Ketzin test site, Germany. *Geochem. Geophys. Geosyst.* 12 (5), 1–10.
- Martens, S., Liebscher, A., Möller, F., Henniges, J., Kempka, T., Lüth, S., Norden, B., Prevedel, B., Szzybalski, A., Zimmer, M., Kühn, M., Ketzin Group, 2013. CO<sub>2</sub> storage at the Ketzin pilot site, Germany: fourth year of injection, monitoring, modelling and verification. *Energy Procedia* 37, 6434–6443, <http://dx.doi.org/10.1016/j.egypro.2013.06.573>.
- Martens, S., Möller, F., Streibel, M., Liebscher, A., the Ketzin Group, 2014. Completion of five years of safe CO<sub>2</sub> injection and transition to the post-closure phase at the Ketzin pilot site. *Energy Procedia* 59, 190–197, <http://dx.doi.org/10.1016/j.egypro.2014.10.366>.
- Michael, K., Golab, A., Shulakova, V., Ennis-King, J., Allinson, G., Sharma, S., Aiken, T., 2010. Geological storage in saline aquifers – a review of the experience from existing storage operations. *Int. J. Greenh. Gas Control* 4, 659–667.
- Norden, B., Frykman, P., 2013. Geological modelling of the Triassic Stuttgart Formation at the Ketzin CO<sub>2</sub> storage site, Germany. *Int. J. Greenh. Gas Control* 19, 756–774, <http://dx.doi.org/10.1016/j.ijggc.2013.04.019>.
- Oreskes, N., Shrader-Frechette, K., Belitz, K., 1994. Verification, validation, and confirmation of numerical models in the earth sciences. *Science* 263, 641–646.
- White, D., 2013. Seismic characterization and time-lapse imaging during seven years of CO<sub>2</sub> flood in the Weyburn field, Saskatchewan, Canada. *Int. J. Greenh. Gas Control* 16 (S1), S78–S94, <http://dx.doi.org/10.1016/j.ijggc.2013.02.006>.
- Würdemann, H., Moeller, F., Kuehn, M., Heidug, W., Christensen, N.P., Borm, G., Schilling, F.R., CO<sub>2</sub>SINK Group, 2010. CO<sub>2</sub>SINK – from site characterisation and risk assessment to monitoring and verification: one year of operational experience with the field laboratory for CO<sub>2</sub> storage at Ketzin, Germany. *Int. J. Greenh. Gas Control* 4 (6), 938–951, <http://dx.doi.org/10.1016/j.ijggc.2010.08.010>.
- Yordkayhun, S., Ivanova, A., Giese, R., Juhlin, C., Cosma, C., 2009. Comparison of surface seismic sources at the CO<sub>2</sub>SINK site, Ketzin, Germany. *Geophysical Prospecting* 57, 125–139, <http://dx.doi.org/10.1111/j.1365-2478.2008.00737.x>.